



2000). Glacial velocity is an important factor influencing ice flux (Rosenau et al., 2012) and an important parameter in the estimation of Antarctic ice sheet mass balance. Additionally, glacial velocity directly signals the response of the Antarctic ice sheet to global climate change. Thus, studies on the velocities of Antarctic glaciers have become important for developing global sea level rise models (Chen et al., 2007).

5 Methods for monitoring Antarctic ice velocities are mainly classified into two categories: in situ measurement and remote sensing monitoring. Stake measurement is the first method of in situ measurement used for monitoring Antarctic ice velocities (Hofmann et al., 1964; Dorrer et al., 1969). At present, global positioning system (hereafter referred to as GPS) technology has become the most important tool for field  
10 measurements of Antarctic glacier dynamics and ice surface terrain (Manson et al., 2000). However, the harsh environment, high cost of field observation, and a relatively short retest period have substantially limited in situ measurements (Urbini, 2008; Sunil, 2007). Remote sensing methods, including microwave and optical remote sensing, allow for rapid development of Antarctic ice velocity measurements using synthetic aperture radar (hereafter referred to as SAR) data (Kimura et al., 2004; Dong et al., 2004; Pattyn and Derauw, 2002). By means of interferometric SAR (hereafter referred to as InSAR) and feature tracking, researchers have obtained ice velocity measurements of the entire Antarctic ice sheet and generated an Antarctic ice sheet velocity profile  
15 (Rignot et al., 2011). SAR data are independent of weather conditions (clouds and rain) and have high accuracy (Ke et al., 2013). Nonetheless, the frequent melting behaviour of glaciers and snow on the Antarctic Peninsula is likely to cause a loss of coherence in SAR images, accounting for the longer observation period of SAR feature tracking method than the InSAR method. Additionally, the impact of incidence angle in steep terrains can limit the visibility of some glaciers in SAR images, and a high-resolution digital elevation model (hereafter referred to as DEM) is needed for terrain correction. Therefore, active microwave remote sensing is highly suitable for velocity monitoring over relatively short periods (Scheuchl et al., 2012).

5877

Co-registration of optically sensed images and correlation (COSI-Corr) is a methodology based on the calculation of grayscale pixel values using a simple algorithm. COSI-Corr is advantageous because of its larger number of optical remote sensors, longer time series, and rich data resources. It is therefore more suitable than SAR  
5 monitoring methods for estimating the speed of glacial movement and the analysis of relevant spatiotemporal variations over long time series (Ferrigno et al., 1998; Liu et al., 2012). Because the accuracy of COSI-Corr is primarily determined by the spatial resolution of a pixel, Antarctic ice sheet velocity monitoring based on optical images mostly adopts high-resolution images, such as TM/ETM (Ferrigno et al., 1994), ASTER (Tiwari et al., 2012), and SPOT (Ahn and Howat, 2010). Additionally, due to differences in the attitudes of satellites, system errors occur during image splicing, and coordination registration errors between different images affect the accuracy of COSI-Corr. Thus, study on cross-correlation algorithms becomes the focus for improving the accuracy of COSI-Corr. For example, Heid and Kaab (2012) compared and evaluated six different  
10 matching algorithms: normalized cross-correlation operated in the spatial domain (NCC), cross-correlation operated in the frequency domain using Fast Fourier Transform (CCF), phase correlation operated in the frequency domain using Fast Fourier Transform (PC), cross-correlation operated in the frequency domain using Fast Fourier Transform on orientation images (CCF-O), phase correlation operated in the frequency domain using Fast Fourier Transform on orientation images (PC-O) and the phase correlation algorithm used in COSI-Corr. The use of high-resolution images for monitoring the velocity of single ice streams on the Antarctic Peninsula has also resulted in important findings. For example, the study by Scambos et al. (2004) estimated the velocities of the Crane Glacier using TM images. As the collapse of the Antarctic ice shelf intensifies, great progress has been made in measuring ice shelf velocities (Yu et al., 2010; Scheuchl et al., 2012). However, few studies have been reported for the Antarctic ice sheet with regard to ice velocities on larger spatial scales over longer time spans.

Antarctic Peninsula glaciers are polar continental glaciers that have high surface velocities (Khazendar et al., 2011). For these glaciers, MODIS data of 250 m resolution

5878









Sea, respectively. At the sea outfall, glaciers are confined by local terrain conditions into thin valley glaciers (ice stream) in diverse flow directions, eventually flowing into ice shelves and the sea (Fig. 7). However, the peninsula's rugged terrain significantly blocks the glacier flow, and the small glacier mass results in weak longitudinal stress of ice flows. Consequently, the Graham Land glaciers as a whole have lower velocities, with a local minimum of  $< 20 \text{ ma}^{-1}$  and a maximum of  $1500 \text{ ma}^{-1}$  (average  $100\text{--}150 \text{ ma}^{-1}$ ). The Larsen Ice Shelf has an average velocity of  $750\text{--}800 \text{ ma}^{-1}$ , with a maximum  $> 1500 \text{ ma}^{-1}$ . Compared with the glaciers of Graham Land, the Larsen Ice Shelf flows in almost a single direction, mainly along the northeast direction into the Weddell Sea. A very large ice flux and less bottom friction account for the significantly higher velocities of the ice shelf than the inland glaciers.

Furthermore, 50 sampling points evenly distributed across Graham Land and the Larsen Ice Shelf have been chosen for more intuitive analysis of the Antarctic Peninsula ice velocity features (Fig. 8). Average velocities at the sampling points are obtained from four sets of inverse velocity contour maps (Fig. 9). As observed, the individual sampling points of Graham Land have discretely distributed velocities, despite their generally low level as a whole. The discrete distribution pattern is possibly the result of the rugged terrain of the narrow Antarctic Peninsula and the differences in ice flux as well as subglacial supporting conditions of the ice shelves. Even the same ice stream at different altitudes has substantial differences in flow velocity. The velocities of ice streams in the upstream regions are relatively low, and the velocities sharply increase when the ice sheet mass converges with numerous tiny ice flows moving toward the sea. For example, the velocities at the upstream reaches of the Crane Glacier are  $< 150 \text{ ma}^{-1}$ , while those near the outfall approach  $1500 \text{ ma}^{-1}$  (Scambos et al., 2004). As for the Larsen Ice Shelf, the sampling points not only have relatively high velocities as a whole but also exhibit more convergent distribution of individual velocities.

5887

## 5.2 Temporal variations in surface velocities

In terms of temporal distribution (Fig. 10), the Graham Land glaciers exhibit complex ice velocity changes at different sampling points. Over the period between 2000 and 2012, the majority of the sampling points showed accelerations, with an average speed increase of 13.5%. This acceleration was slightly higher than that reported by Pritchard et al. (2007), who estimated an average speed increase of 12% for more than 300 glaciers during 1992–2005. The acceleration was mainly because rapid disintegration of the Larsen Ice Shelf in large areas led to rapid flow of the upstream-supplied glaciers. In particular, the large-scale disintegration of the Larsen B Ice Shelf at the end of the last century caused a speed increase of 35% in the upstream Crane Glacier over the period 2000–2012. In addition, surface melting and massive bottom melting near the grounding line contributed to the acceleration of the ice sheet flows (Rignot et al., 2008). Generally speaking, glacial acceleration is a common phenomenon in the Antarctic. For example, the Thwaites Glacier Tongue accelerated from  $2680 \text{ ma}^{-1}$  over the period 1972–1984 to  $2950 \text{ ma}^{-1}$  in 2006 (Rosanova et al., 1998), whereas the Haynes and Smith glaciers accelerated by 27 and 75%, respectively, from 1996 to 2006. In particular, the Smith Glacier experienced a speed increase by 8% over the one-year period 2006–2007 (Rignot, 2008). In the northern part of the peninsula, there were five sampling points associated with a decrease in the average velocity. The slowdown was possibly related to strong, rapid thinning of the ice sheet mass in local areas. Mass reduction can cause weakening of the longitudinal stress and thus lead to unexpected slowdown. This slowdown feature is also present in the Siple Coast C ice streams and the Whillans ice streams (Bindschadler et al., 1996).

The sampling points on the Larsen Ice Shelf clearly accelerated over time, with an average velocity increase of 13% from 2000 to 2006 and 15% from 2006 to 2012. These speed increases were greater than those estimated for the period 1988–1994 and 1994–1997, i.e. 13.2% (Kvarcaet et al., 1999). Our results coincided with previous estimates of the change pattern by Vieli et al. (2006), who reported that the Larsen B

5888

shelf accelerated by  $150 \text{ m a}^{-1}$  from 1995–1999. It is due mainly to rapid disintegration of the ice shelf itself that led to the faster flowing ice streams (Stephenson and Bindshadler, 1988; Rignot et al., 2008).

### 5.3 Error analysis

5 Due to restrictions of natural conditions, less in situ measurement data are available for the Antarctic Peninsula. The results obtained using remote sensing methods are mainly focused on single glaciers (ice streams). In the present study, the average velocity, i.e.  $850\text{--}1350 \text{ m a}^{-1}$  of the downstream Crane Glacier in 2002–2003 is estimated based on MODIS data (Fig. 11). This result is consistent with the estimate of  
10 downstream Crane Glacier in 2001–2002 based on TM images, i.e.  $950\text{--}1500 \text{ m a}^{-1}$  (Scambos et al., 2004). As for individual ice streams, velocity estimation based on MODIS data has slightly lower accuracy. However, the average velocity of the Larsen B Ice Shelf during 2000–2012 is estimated to be  $350\text{--}450 \text{ m a}^{-1}$  (Fig. 12), which coincides with the results previously estimated using high-resolution image data, i.e. an  
15 average velocity of  $370 \text{ m a}^{-1}$  during 2002–2006 and an acceleration of  $400 \text{ m a}^{-1}$  from 2006 to 2009 (Haug et al., 2010; Scambos et al., 2004).

The velocity-estimation method of a single glacier used in this study has relatively low accuracy relative to other methods such as high-resolution optical image feature tracking (Lucchitta and Rosanova, 1997; Frezzotti et al., 1998), InSAR (Fricker et al.,  
20 2009), and GPS. However, this method can still achieve satisfactory results in open areas of ice shelf regions that have significant flowing texture. Nonetheless, there are a few constraints for this method.

With regard to image quality, the Antarctic Peninsula experiences frequent mass exchange with the ocean, leading to cloudy, snowy weather almost year-round. It is therefore  
25 very difficult to obtain optical images of high quality for cross-correlation calculations. Here, we chose cross-correlation images with  $< 10\%$  cloud cover from massive quantities of data from 2000, 2003, 2006, 2009, and 2012. However, the cloud cover

5889

conditions in local areas are not ideal, affecting the accuracy of the regional feature tracking to some extent.

From the perspective of feature point defects, the correlation calculation of glacier movement mainly involves moraine deposits, ice cracks, crevasses, and ice mounds.  
5 As indicated above, the surface of the Antarctic ice sheet is very uniform with much fewer moraines than valley glaciers. Additionally, a large amount of snow accumulates on the glacier surface, which can cover surface feature points (Esra et al., 2009). Compared with valley glaciers, ice shelf regions lack evident textural features due to the flat terrain and very large ice stream mass. Moreover, false matching of feature points may  
10 occur in ice shelves due to vertical variations caused by freeze-melt and seawater tides (Yu et al., 2010).

Another possible source of error may be related to the micro-terrain. The terrain of the Antarctic Peninsula is rugged, forming many small ice streams, such as the Hektor and Green glaciers. Their widths only occupy a few pixels of the MODIS images, whereas the grid segmentation of the cross-correlation calculation requires a certain  
15 number of pixels to ensure accuracy. Hence, feature tracking based on medium-resolution optical images may be ineffective for velocity estimation of very small ice streams of the Antarctic ice sheet (Scherler et al., 2008).

The above limitations can impact the accuracy of the glacier surface velocity estimation for the Antarctic Peninsula, resulting in abnormal velocities at a few sampling points (Fig. 9). However, CCC algorithm using medium-resolution optical images is a very useful tool in studying the spatiotemporal variations in large-scale glacier movement in the Antarctic ice sheet area.  
20

## 6 Conclusions

25 This study estimates glacier velocities in the Antarctic Peninsula using COSI-Corr based on MODIS L1B data from years 2000, 2003, 2006, 2009, and 2012. The results show that the Graham Land glaciers and the Larsen Ice Shelf have distinctive velocity

features. The glaciers of Graham Land as a whole have low velocities, with an average of  $100\text{--}150\text{ m a}^{-1}$ . Due to the rugged nature of the underlying terrain and different quantities of glacier mass, there are tremendous differences in ice velocities among the Graham Land glaciers, as reflected by a maximum of approximately  $1500\text{ m a}^{-1}$  and a minimum of  $< 20\text{ m a}^{-1}$ . As for the Larsen Ice Shelf, the overall velocity is relatively high due to the very large ice flux and lower bottom friction near the grounding line. The Larsen Ice Shelf has an average velocity of  $750\text{--}800\text{ m a}^{-1}$  with a maximum of  $> 1500\text{ m a}^{-1}$ , making it one of the fastest-moving regions in the Antarctic ice sheet. The Graham Land glacier velocities experienced complex changes over time. Due to downstream glacier mass loss, the average velocity increased by 13.5 % from 2000 to 2012 in the southern part of the Peninsula. Certain glaciers even accelerated by 30 %, whereas local areas in the northern part of the peninsula experienced velocity decreases. The latter phenomenon could be related to the reduction of longitudinal stress caused by the rapid thinning of glaciers. In recent years, the Larsen Ice Shelf has rapidly disintegrated on a large scale. Together, glacier surface melt and strong bottom melting (Rignot et al., 2008) near the grounding line have contributed to the acceleration of ice shelves and upstream-supplied glaciers. The average velocity of the Larsen Ice Shelf increased by 13 % from 2000 to 2006 and by 15 % from 2006 to 2012.

MODIS data can be used to continuously monitor the glacier surface velocities of the Antarctic Peninsula over large spatial scales and for long time series. MODIS L1B has clear advantages in large-scale macroscopic research of spatiotemporal variations in the Antarctic ice sheet movement. Satisfactory results are estimated especially for the Larsen Ice Shelf. However, due to issues related to clouds, feature point defects, micro-terrain, and the simplicity of the CCC algorithm, certain level of errors occur in the velocity estimates of the Graham Land glaciers.

*Acknowledgements.* This work was supported by Program for National Nature Science Foundation (No. 41371391), Program for Chinese National Antarctic and Arctic Research Expedition (CHINARE2014-02-02), Program for the Specialized Research Fund for the Doctoral Program of Higher Education of China (No. 20120091110017) and A Project Funded by the

5891

PriorityAcademicProgram Development of Jiangsu Higher Education Institutions (PAPD). And this work was partially supported by Collaborative Innovation Center of Novel Software Technology and Industrialization.

## References

- Ahn, Y. and Howat, I. M.: Efficient automated glacier surface velocity measurement from repeat images using multi-image/multichip and null exclusion feature tracking, *IEEE T. Geosci. Remote*, 49, 2838–2846, doi:10.1109/TGRS.2011.2114891, 2010.
- Bamber, J. L., Riva, R. E. M., Vermeersen, B. L. A., and LeBrocq, A. M.: Reassessment of the potential sea-level rise from a collapse of the West Antarctic Ice Sheet, *Science*, 324, 901–903, doi:10.1126/science.1169335, 2009.
- Berthier, E., Raup, B., and Scambos, T. A.: New velocity map and mass-balance estimate of Mertz Glacier, East Antarctica, derived from Landsat sequential imagery, *J. Glaciol.*, 49, 503–511, doi:10.3189/172756503781830377, 2003.
- Brown, L. G.: A survey of image registration techniques, *Comput. Surv.*, 24, 325–376, doi:10.1145/146370.146374, 1992.
- Bindschadler, R. A., Vornberger, P., Blankenship, D., Scambos, T. A., and Jacobel, R.: Surface velocity and mass balance of Ice Streams D and E, West Antarctica, *J. Glaciol.*, 42, 461–475, 1996.
- Bindschadler, R. A., Scambos, T. A., Rott, H., Skvarca, P., and Vornberger, P.: Ice dolines on Larsen Ice Shelf, Antarctica, *Ann. Glaciol.*, 34, 283–290, doi:10.3189/172756402781817996, 2002.
- Cheng, X., Li, X., Shao, Y., and Li, Z.: DINSAR measurement of glacier motion in Antarctic Grove Mountain, *Chinese Sci. Bull.*, 52, 358–366, doi:10.1007/s11434-007-0054-y, 2007.
- Djamel, A. and Hammadi, A.: External Validation of the ASTER GDEM2, GMTED2010 and CGIAR-CSI-SRTM v4.1 free access Digital Elevation Models (DEMs) in Tunisia and Algeria, *Remote Sens.*, 6, 4600–4620, doi:10.3390/rs6054600, 2014.
- Dong, C. E., Zhou, C. X., and Liao, M. S.: Application of SAR interferometry in Grove Mountains, East Antarctica, *Ann. Glaciol.*, 23, 514–521, doi:10.1117/12.514161, 2004.
- Dorrer, E., Hofmann, W., and Seufert, W.: Geodetic results of the Ross Ice Shelf survey expeditions, 1962–1963 and 1965–1966, *J. Glaciol.*, 52, 67–90, 1969.

5892

- Dyurgerov, B. and Meier, M. F.: Twentieth century climate change: evidence from small glaciers, *P. Natl. Acad. Sci. USA*, 97, 1406–1411, doi:10.1073/pnas.97.4.1406, 2000.
- Erten, E., Chesnokova, O., Hajnsek, I., and Reigber, A.: Glacier surface velocity measure based on polarimetric tracking, *Ann. Glaciol.*, 12, 3126–3129, doi:10.1109/IGARSS.2012.6350763, 2012.
- Esra, E., Andreas, P., Olaf, H., and Pau, P.: Glacier velocity monitoring by maximum likelihood texture tracking, *IEEE T. Geosci. Remote*, 47, 394–405, doi:10.1109/TGRS.2008.2009932, 2009.
- Evans, A. N.: Glacier surface motion computation from digital image sequences, *IEEE T. Geosci. Remote*, 38, 1064–1072, doi:10.1109/36.841985, 2000.
- Ferrigno, J. G., Mullins, J. L., Stapleton, J. A., Bindschadler, R. A., Scambos, T. A., Bellissime, L. B., Bowell, J. A., and Acosta, A. V.: Landsat TM image maps of the Shirase and Siple Coast Ice Streams, West Antarctica, *Ann. Glaciol.*, 20, 407–412, doi:10.3189/172756494794587087, 1994.
- Ferrigno, J. G., Williams, R. S., Rosanova, C. E., Lucchitta, B. K., and Swithbank, C.: Analysis of coastal change in Marie Byrd Land and Ellsworth Land, West Antarctica, using Landsat imagery, *Ann. Glaciol.*, 27, 33–40, 1998.
- Frezzotti, M. A., Capra, A., and Vittuari, L.: Comparison between glacier ice velocities inferred from GPS and sequential satellite images, *Ann. Glaciol.*, 27, 54–60, 1998.
- Fricker, H. A., Coleman, R., Padman, L., Scambos, T. A., Bohlander, J., and Brunt, K. M.: Mapping the grounding zone of the Amery Ice Shelf, east Antarctica using InSAR, MODIS and ICESat, *Antarct. Sci.*, 21, 515–532, doi:10.1017/S095410200999023X, 2009.
- Haug, T., Käab, A., and Skvarca, P.: Monitoring ice shelf velocities from repeat MODIS and Landsat data – a method study on the Larsen C ice shelf, Antarctic Peninsula, and 10 other ice shelves around Antarctica, *The Cryosphere*, 4, 161–178, doi:10.5194/tc-4-161-2010, 2010.
- Heid, T. and Käab, A.: Evaluation of existing image matching methods for deriving glacier surface displacements globally from optical satellite imagery, *Remote Sens. Environ.*, 118, 339–355, doi:10.1016/j.rse.2011.11.024, 2012.
- Hofmann, W., Dorrer, E., and Nottarp, K.: The Ross Ice Shelf survey (RISS) 1962–1963, in *Antarctic snow and ice studies*, *J. Glaciol.*, 45, 83–117, 1964.

5893

- Holger, F. and Frank, P.: On the suitability of the SRTM DEM and ASTER GDEM for the compilation of topographic parameters in glacier inventories, *Int. J. Appl. Earth Obs.*, 18, 480–490, doi:10.1016/j.jag.2011.09.020, 2012.
- Huang, L. and Li, Z.: Mountain glacier flow velocities analyzed from satellite optical images, *J. Glaciol. Geocryol.*, 31, 935–940, 2009.
- Huang, L. and Li, Z.: Comparison of SAR and optical data in deriving glacier velocity with feature tracking, *Int. J. Remote Sens.*, 33, 2681–1698, doi:10.1080/01431161003720395, 2011.
- Käab, A., Lefauconnier, B., and Melvold, K.: Flow field of Kronebreen, Svalbard, using repeated Landsat 7 and ASTER data, *Ann. Glaciol.*, 42, 7–13, doi:10.3189/172756405781812916, 2005.
- Kang, X. W. and Feng, Z. K.: An introduction to ASTER GDEM and procedure reading, *Appl. Remote Sens.*, 6, 69–72, 2011.
- Ke, C. Q., Kou, C., Ludwig, R., and Qin, X.: Glacier velocity measurements in the eastern Yigong Zangbo basin, Tibet, China, *J. Glaciol.*, 59, 1060–1068, doi:10.3189/2013JoG12J234, 2013.
- Khazendar, A., Rignot, E., and Larour, E.: Acceleration and spatial rheology of Larsen C Ice Shelf, Antarctic Peninsula, *Geophys. Res. Lett.*, 38, L09502, doi:10.1029/2011GL046775, 2011.
- Kimura, H., Kanamori, T., Wakabayashi, H., and Nishio, F.: Ice sheet motion in inland Antarctica from JERS-1 SAR interferometry, *Int. Geosci. Remote Se.*, 1–7, 3018–3020, doi:10.1109/IGARSS.2004.1370332, 2004.
- Liu, H. X., Wang, L., Tang, S. J., and Jezek, K. C.: Robust multi-scale image matching for deriving ice surface velocity field from sequential satellite images, *Int. J. Remote Sens.*, 33, 1799–1822, doi:10.1080/01431161.2011.602128, 2012.
- Lucchitta, B. K. and Rosanova, C. E.: Velocities of Pine Island and Thwaites Glaciers, West Antarctica, from ERS-1 SAR images, *Ann. Glaciol.*, 21, 819–824, 1997.
- Lucchitta, B. K., Mullins, K. F., Allison, A. L., and Ferrigno, J. G.: Antarctic glacier-tongue velocities from Landsat images-1st result, *Ann. Glaciol.*, 27, 356–366, 1993.
- Manson, R., Coleman, R., Morgan, P., and King, M.: Ice velocities of the Lambert Glacier from static GPS observations, *Earth Planets Space*, 52, 1031–1036, 2000.

5894

- Meredith, M. P. and King, J. C.: Rapid climate change in the ocean west of the Antarctic Peninsula during the second half of the 20th century, *Geophys. Res. Lett.*, 32, L19604, doi:10.1029/2005GL024042, 2005.
- Ni, W. J., Zhang, Z. Y., Sun, G. Q., Guo, Z. F., and He, Y. T.: The penetration depth derived from the synthesis of ALOS/PALSAR InSAR data and ASTER GDEM for the mapping of forest biomass, *Remote Sens.*, 6, 7303–7319, doi:10.3390/rs6087303, 2014.
- Osmanoglu, B.: Surface velocity and ice discharge of the ice cap on King George Island, Antarctica, *Ann. Glaciol.*, 54, 111–119, doi:10.3189/2013AoG63A517, 2013.
- Pattyn, F. and Derauw, D.: Ice–dynamic conditions of Shirase Glacier, Antarctica, inferred from ERS SAR interferometry, *J. Glaciol.*, 48, 559–565, doi:10.3189/172756502781831115, 2002.
- Pritchard, H. D. and Vaughan, D. C.: Widespread acceleration of tide water glaciers on the Antarctic Peninsula, *J. Geophys. Res.*, 112, 1029–1031, doi:10.1029/2006JF000597, 2007.
- Rack, W., Rott, H., Siegel, A., and Skvarca, P.: The motion field of northern Larsen Ice Shelf, Antarctic Peninsula, derived from satellite imagery, *Ann. Glaciol.*, 29, 261–266, doi:10.3189/172756499781821120, 1999.
- Rosanova, C. E., Lucchitta, B. K., and Ferrigno, J. G.: Velocities of Thwaites Glacier and smaller glaciers along the Marie Byrd Land coast, West Antarctica, *Ann. Glaciol.*, 27, 47–53, 1998.
- Rosenau, R., Dietrich, R., and Baessler, M.: Temporal flow variations of major outlet glaciers in Greenland using Landsat data, *Int. Geosci. Remote Se.*, 23, 1557–1560, doi:10.1109/IGARSS.2002.1025771, 2002.
- Rignot, E.: Changes in west Antarctic ice stream dynamics observed with ALOS PALSAR data, *Geophys. Res. Lett.*, 35, 63–74, doi:10.1029/2008GL033365, 2008.
- Rignot, E., Casassa, G., and Gogineni, S.: Accelerated ice discharge from the Antarctic Peninsula following the collapse of Larsen B ice shelf, *Geophys. Res. Lett.*, 32, 1–4, doi:10.1029/2004GL020697, 2004.
- Rignot, E., Bamber, J. L., Van Den Broeke, M. R., Davis, C., Li, Y. H., Van De Berg, W. J., and Van Meijgaard, E.: Recent Antarctic ice mass loss from radar interferometry and regional climate modelling, *Nat. Geosci.*, 1, 106–110, doi:10.1038/ngeo102, 2008.
- Rignot, E., Mouginot, J., and Scheuchl, B.: Ice flow of the Antarctic Ice Sheet, *Science*, 9, 1427–1430, doi:10.1126/science.1208336, 2011.

5895

- Saraswat, P., Syed, T. H., Famiglietti, J. S., Fielding, E. J., Crippen, R., and Gupta, N.: Recent changes in the snout position and surface velocity of Gangotri glacier observed from space, *Int. J. Remote Sens.*, 34, 8653–8668, doi:10.1080/01431161.2013.845923, 2013.
- Scambos, T. A., Dutkiewicz, M. J., Wilson, J. C., and Bindschadler, R. A.: Application of image cross-correlation to the measurement of glacier velocity using satellite image data, *Remote Sens. Environ.*, 42, 177–186, doi:10.1016/0034-4257(92)90101-O, 1992.
- Scambos, T. A., Bohlander, J. A., Shuman, C. A., and Skvarca, P.: Glacier acceleration and thinning after ice shelf collapse in the Larsen B embayment, Antarctica, *Geophys. Res. Lett.*, 31, L18402, doi:10.1029/2004GL020670, 2004.
- Scherler, D., Leprince, S., and Strecker, M. R.: Glacier-surface velocities in alpine terrain from optical satellite imagery—Accuracy improvement and quality assessment, *Remote Sens. Environ.*, 112, 3806–3819, doi:10.1016/j.rse.2008.05.018, 2008.
- Scheuchl, B., Mouginot, J., and Rignot, E.: Ice velocity changes in the Ross and Ronne sectors observed using satellite radar data from 1997 and 2009, *The Cryosphere*, 6, 1019–1030, doi:10.5194/tc-6-1019-2012, 2012.
- Shi, Y. F. and Liu, S. Y.: Chinese glacier response to global warming in the 21st century estimate, *Chinese Sci. Bull.*, 45, 434–438, 2000.
- Skvarca, P., Rack, W., and Rott, H.: 34 year satellite time series to monitor characteristics, extent and dynamics of Larsen B Ice Shelf, Antarctic Peninsula, *Ann. Glaciol.*, 29, 255–260, doi:10.3189/172756499781821283, 1999.
- Slater, J. A., Heady, B., Kroenung, G., Curtis, W., Haase, J., Hoegemann, D., Shockley, C., and Tracy, K.: Evaluation of the New ASTER Global Digital Elevation Model, National Geospatial-Intelligence Agency, Springfield, VA, USA, 2009.
- Stephenson, S. N. and Bindschadler, R. A.: Observed velocity fluctuations on a major Antarctic ice stream, *Nature*, 334, 695–697, doi:10.1038/334695a0, 1988.
- Sunil, P. S.: GPS determination of the velocity and strain–rate fields on Schirmacher Glacier, central Dronning Maud Land, Antarctica, *J. Glaciol.*, 53, 558–564, doi:10.3189/002214307784409199, 2007.
- Tiwari, R. K., Gupta, R. P., and Arora, M. K.: Estimation of surface ice velocity of Chhota-Shigri glacier using sub-pixel ASTER image correlation, *Curr. Sci. India*, 106, 853–859, 2014.
- Turner, J., Colwell, S. R., Marshall, G. J., Lachlan-Cope, T. A., Carleton, A. M., Jones, P. D., Lagun, V., Reid, P. A., and Iagovkina, S.: Antarctic climate change during the last 50 years, *Int. J. Climatol.*, 25, 279–294, doi:10.1002/joc.1130, 2005.

5896



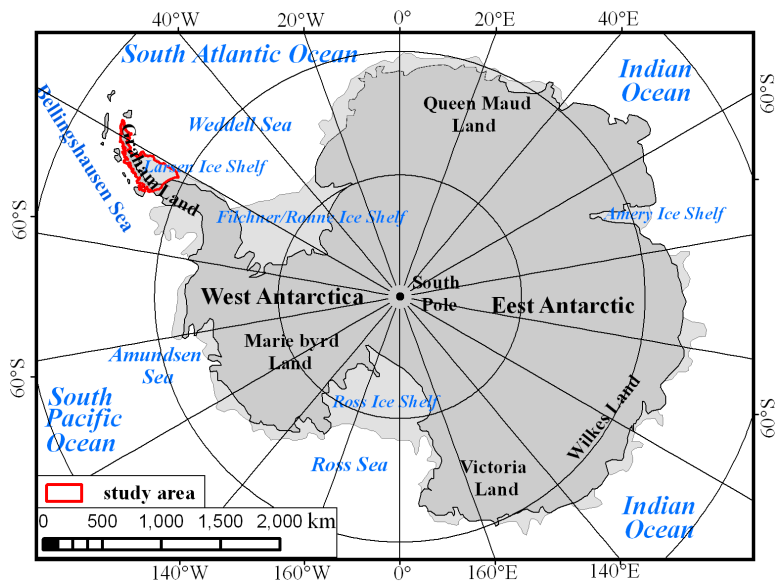


Figure 1. Location of the study area.

5899

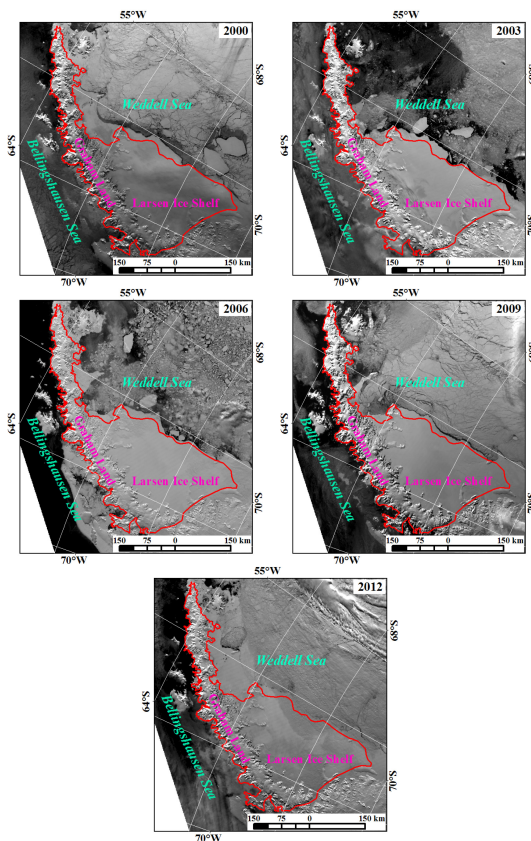
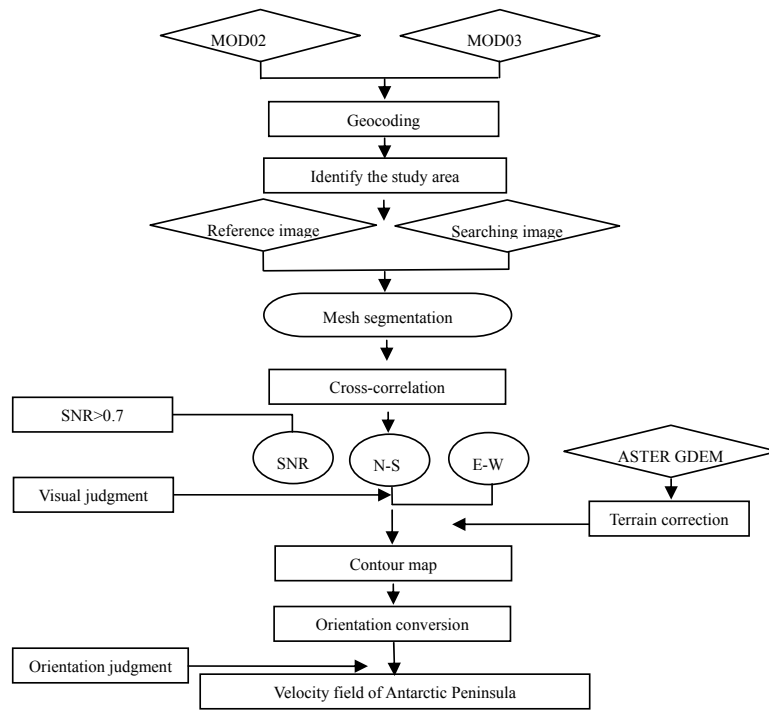


Figure 2. The melt line of the Antarctic Peninsula in different years.

5900



**Figure 3.** Processing flowchart for deriving glacier surface flow velocities.

5901

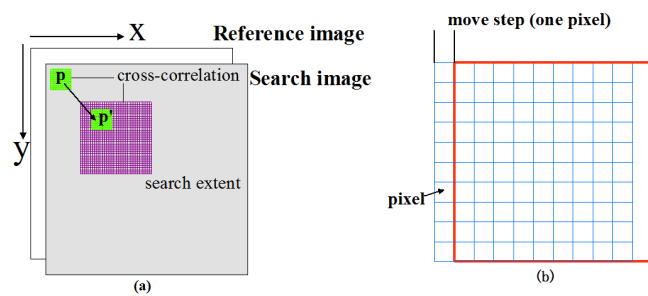


**Figure 4.** Sketch map of feature tracking.

5902

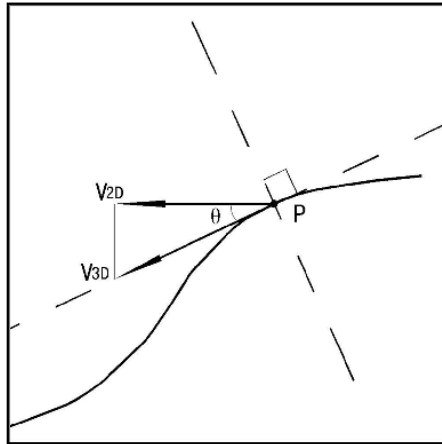


**Figure 5.** Horizontal velocity and actual velocity of the glacier surface.

5903

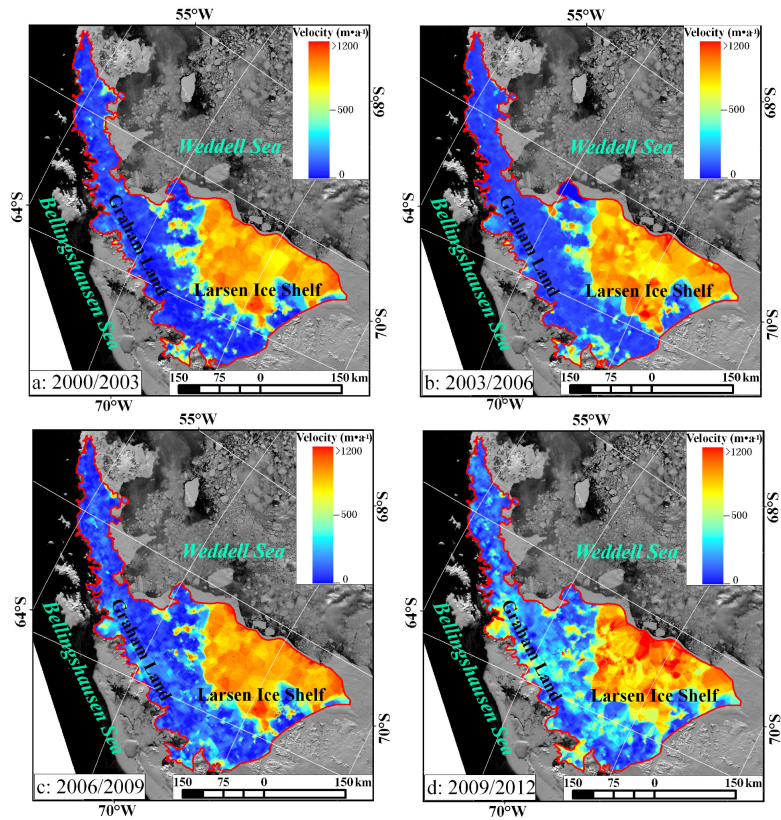


**Figure 6.** The glacier surface velocity of Antarctic Peninsula.

5904

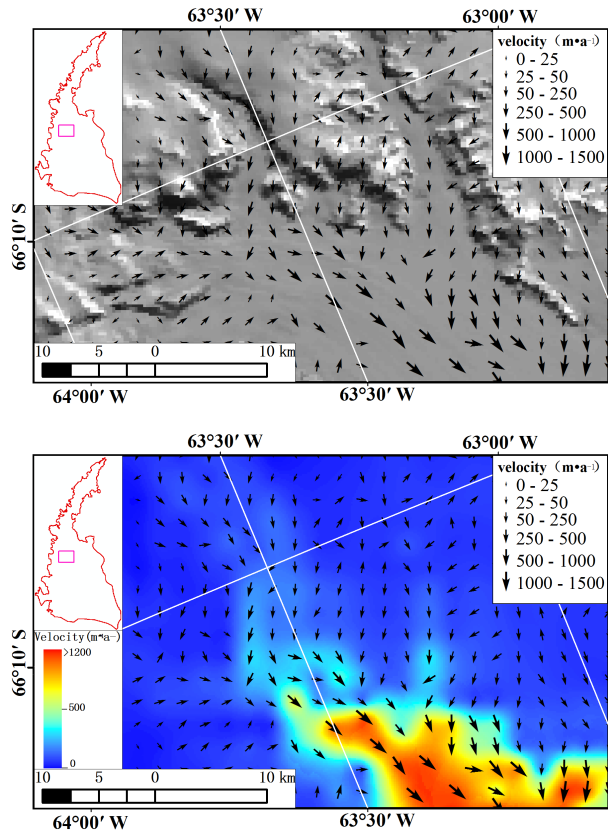


Figure 7. Velocity field of the Antarctic Peninsula (2000/2003).

5905

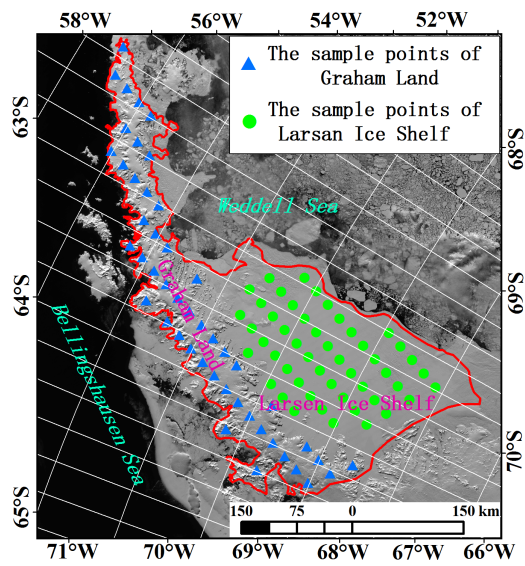
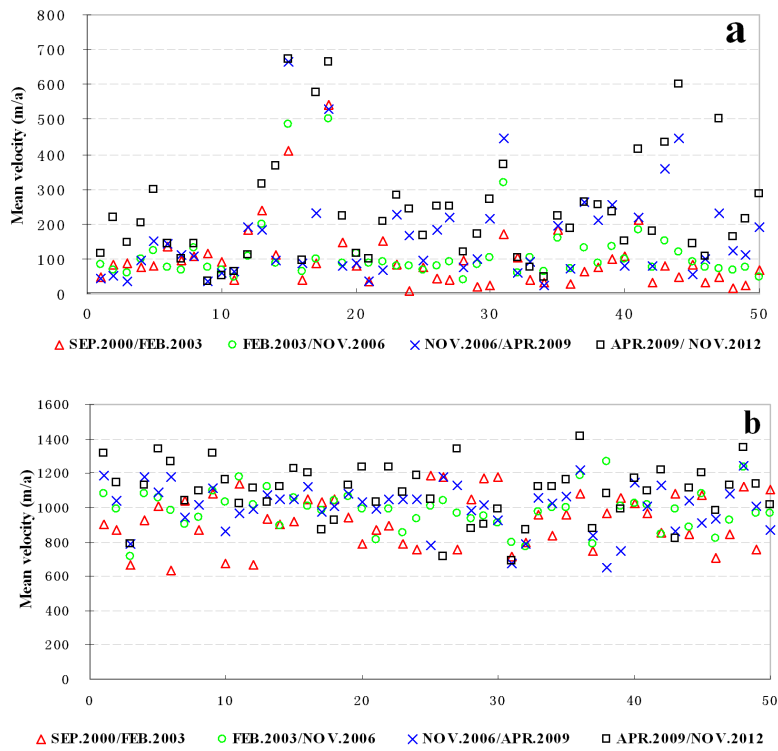


Figure 8. Sketch map of the 50 sample points.

5906



**Figure 9.** Average annual velocity of the 50 sample points. **(a)** Graham Land, **(b)** Larsen Ice Shelf.

5907

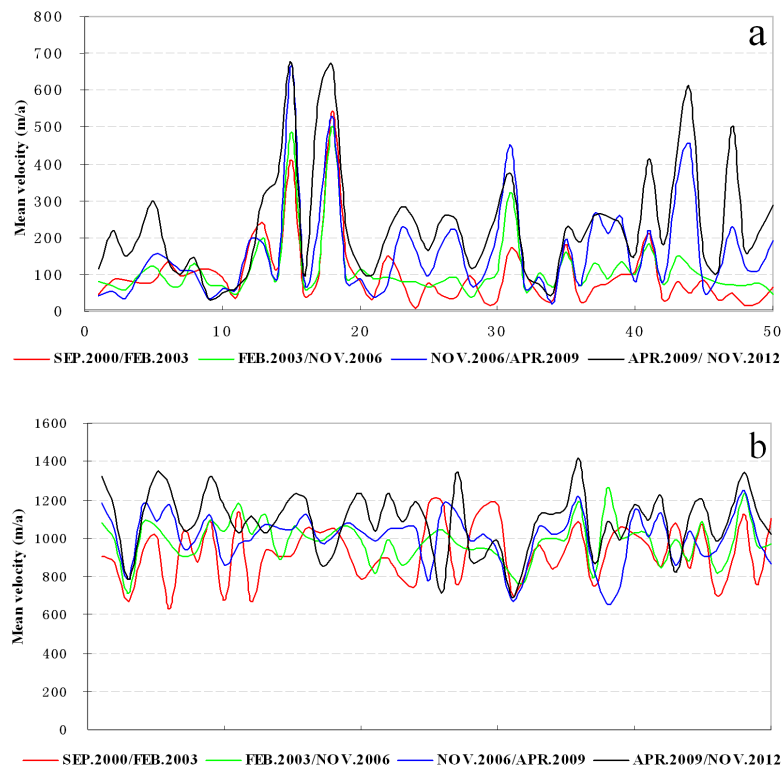


**Figure 10.** The changing average annual velocities, **(a)** Graham Land, **(b)** Larsen Ice Shelf.

5908

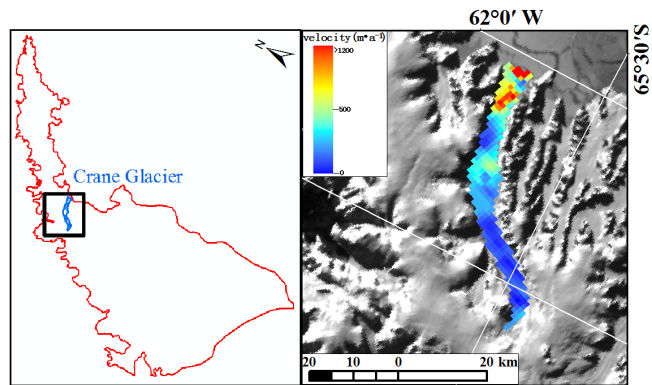


**Figure 11.** Location of the Crane Glacier and average annual velocity of the Crane Glacier from 2000 to 2003.

5909

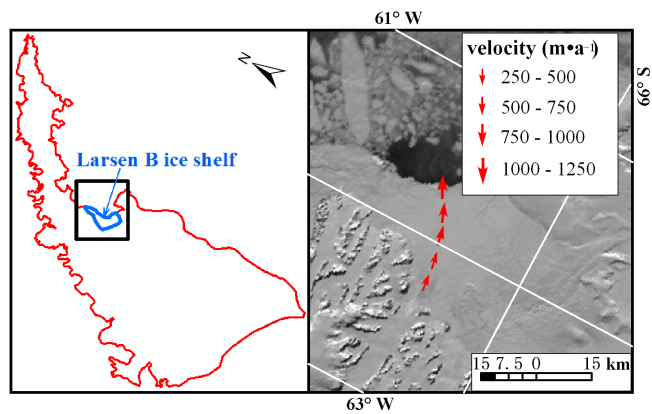


**Figure 12.** Location of the Larsen B ice shelf and Average annual velocity of the Larsen B ice shelf from 2000 to 2012.

5910